JTTEES 2:351-356

Grinding Induced Effects in Plasma Sprayed Zirconia Coatings

J. Zeman, M. Cepera, J. Musil, and J. Filipensky

The effect of grinding on the surface layer properties of ceria and yttria partially stabilized zirconia plasma-sprayed coatings (CePSZ, YPSZ, respectively) has been studied by X-ray diffraction methods. For this purpose, the modified model of line broadening analysis has been derived. The model considers elastic anisotropic properties along with more random paracrystal imperfections, both affecting X-ray line broadening. Grinding-induced microstructural changes were also studied using an estimation from the quantitative Orientation Distribution Function (ODF) texture. It was concluded, based on this work, that CePSZ ceramic is less mechanically stable compared to YPSZ. Consequently, more beneficial mechanical properties of a ground surface layer can be expected for CePSZ plasma-sprayed coatings.

1. Introduction

CERIA and yttria partially stabilized zirconia (CePSZ, YPSZ, respectively) are unstable under the influence of pressure. This behavior is beneficial with regard to mechanical properties, especially the fracture toughness of plasma-sprayed ceramic coatings.[1]

It was observed for monocrystals[2] that external plane-strain loading introduced by surface grinding increased the XRD peak intensity ratios of the $I_{(002)}/I_{(200)}$ and $I_{(113)}/I_{(311)}$ couples. It was concluded[3] that the surface stress state could alter the crystal domain orientation so that the *c*-axes were oriented orthogonal to the surface. Evidence of YPSZ microstructural changes and interpretations based on phase transformations and ferroelastic domain switching mechanisms have been reported.[4-6] The effect of temperature up to 2100 °C and compressive loading at 2.25 GPa were also studied. The effect of biaxial compressive stress loading was nearly the same in both cases, although the X-ray diffraction peak intensity ratios, influenced by higher temperatures, were markedly increased.

The work of Wadhawan[3] concerns the ferroelasticity phenomena and related crystal structures. Most works (including Ref 4 and 5) focus on interpretation of XRD techniques. However, they are not applied to thin ceramic plasma-sprayed coatings, as detailed below. The microstructural heterogeneity arising from the thermal spray process produces a broad range of grain sizes and imperfections such as voids, pores, and microcracks. Also, the X-ray penetration depth is restricted to several micrometers, which might be unrepresentative of the entire coating. Finally, the texture of the coating could be a source of error with regards to quantitative phase analyses.

On the other hand, however, the low X-ray penetration depth can provide suitable conditions for studying grinding-induced effects due to the loading of the top surface. In such cases, further analysis of surface residual stresses as well as microdistortions and the level of paracrystallinity can be measured.[11] The term of "paracrystallinity" is used in this article to describe the statistical representation of long-range order imperfections.[12]

A texturing effect due to directional external stress fields would be expected; likewise, the existence of a texture in the as-deposited coating cannot be omitted. It is evident[13] that the texture, as evaluated by the Orientation Distribution Function (ODF), is a very sensitive tool that can recognize changes in relevant technological factors.

The objective of the present work was to establish direct experimental evidence of ferroelastic domain switching and related properties in plasma-deposited YPSZ and/or CePSZ ceramics. As-received and ground materials were analyzed.

Key Words: grinding, machining, phase transformations, X-ray diffraction, zirconia

J. Zeman and **M. Cepera,** Materials and Technology Institute, P.O. Box 547, 602 00 Brno, Czech Republic; and **J. Musil** and **J. Filipensky,** Plasmacentrum Ltd. Prague, z-01 Brno, Purkynova 118, 612 00 Brno, Czech Republic.

2. Experimental Methods

2.1 *Residual Stress Measurement*

The low X-ray penetration depth due to a high absorption and general heterogeneity problems imply that the $\sin^2\varphi$ relationship commonly used to analyze macroscopic stresses is ineffective and/or misleading for plasma-sprayed coatings. An alternative method, which assumed a residual strain estimation of $\varepsilon = (d_i - d_o)/d_o$ normal to the surface, was therefore chosen to be a more appropriate approach. The terms d_i and d_o are the interplanar spacings of measured and standard specimens, respectively. When the different diffraction peaks ranging the full 2θ angle scale are taken into account, then the effect of different X-ray penetration depths as well as possible elastic strain gradients can be observed.

2.2 *Microstrain and Paracrystallinity*

The microstructure of plasma-sprayed ceramic coatings is highly defective, and therefore, technical difficulties are encountered in defining the macroscopic residual stress field. Thus, an assessment of the microstrain level or any other pa-

rameter that describes the density of defects on an atomic scale is useful, although it will only be on a relative scale.

Microstrain can be estimated using the relation of X-ray diffraction integral peak widths, following the Warren and Biscoe relationship:[7,8]

$$[b(2\theta)]^2 = [\lambda / D_I \cos(\theta)]^2 + [4\varepsilon_I \tan(\theta)]^2 \quad [1]$$

where b is the integral diffraction peak width; λ is the X-ray wave length; θ is the diffraction angle; D_I is the mean domain size; and ε_I is microstrain. The application of this relation to plasma-sprayed coatings is difficult, because no crystal plane systems have the required XRD intensity of higher order diffraction peaks, as is required by a conservative approach. Moreover, the statistical accuracy of such an estimation is usually poor due to the low number of data points.

Substituting ε_I in Eq 1:

$$\left|\varepsilon_I(hkl)\right| = \left|\sigma_L[(xS^{\sigma}_{hkl}) + (1-x)S^{\varepsilon}]\right|$$

$$\left|\varepsilon_I(hkl)\right| = \left|\sigma_L S^{\sigma}_{hkl}\right| \quad [2]$$

where σ_L is microstress averaged over the column of L length; S^{σ}_{hkl} and S^{ε} are the elastic moduli according to Reuss and Voigth approximations,[9] and x is a mixing factor.

The modified relation (Eq 2) enables a rigorous statistical estimation that uses all of the well-defined diffraction peaks from the given spectra, but it is necessary to know the anisotropic elastic moduli of the material. The theory of paracrystals[11,12] expresses the relationship shown in Eq 1 as follows:

$$b^* \cos(\theta)/\lambda = 1/L + 2\pi^2 g^2_{hkl} \sin(\theta)/\lambda \quad [3]$$

in which b^* represents the integral width; L is the mean domain size; and g_{hkl} is a paracrystal distortion parameter.[11]

As in Eq 1, the use of Eq 3 depends on whether the data pertinent to the same crystal system planes; i.e., that of several different orders of crystal systems, are available.

It is postulated that the measured line broadening for rigid polycrystal aggregates is a superposition of two main effects. The first is an elastic distortion component (B_ε) due to the compatibility of a crystal in a compact crystal aggregate. The second more stable component (B_p) arises from the defect distribution in the sense of paracrystal theory. Both the elastic and stable components are, for the sake of simplicity, assumed to be additive following the relation:

$$[B^*]^2 = [B^2_p] + [B^2_\varepsilon] \quad [4]$$

The resultant relationship can be written as:

$$\left\{B^*_{hkl} \cos(\theta)\right\}^2 = (\lambda/L)^2 + (2\pi^2[g^2_p])^2 \sin(\theta)^2 + (4\sigma_L)^2(S_{hkl} \sin(\theta))^2 \quad [5]$$

The unknown parameters of Eq 5, i.e., L, g_p, and σ_L, with their error estimation would be obtained using multiple regression statistics of all of the diffraction peaks from the given spectra. In the case of the present work, however, some selection according to the accuracy in separating superimposed tetragonal doublets must be carried out. A simplified model results from the pragmatic compromise between a true solid physics approach and the experimental accuracy available for the ceramic materials being studied.

2.3 *Quantitative Texture Assessment*

The existence of a crystallographic texture in ceramic coatings was verified for zirconia stabilized by 8% Y_2O_3 and/or 20% CeO_2.[13]

The texture formation results from the processes where partially or completely melted ceramic particles impact against the substrate and then crystal growth occurs due to a preferred direction of heat flow. The texture, in the absence of another factor, is mainly normal to the surface direction. Phase transformations in a solid solution cannot then completely eliminate the texture originally formed, but its character, i.e., ideal crystal orientation and volume content of some texture component, might exhibit a general change. The quantitative assessment of the given texture using X-ray diffraction and its ODF[15] was then applied to the experimental program presented here.

3. Experimental Conditions

The two materials used were 8 wt% Y_2O_3 stabilized ZrO_2 (YPSZ) (Plasmatex 1085) and 18 wt% CeO_2-stabilized ZrO_2 (CePSZ). The grain size of both materials was in the range of 10 to 60 μm. Plasma spray conditions for both materials using Plasma-Technik A 2000 equipment, were as follows: plasma gases of argon/hydrogen at flow rates of 36/11 l/min, a current of 550 A, and a spraying distance of 120 mm. In the case of the YPSZ material, another set of coatings was also prepared (YPSZ-R) to simulate conditions of lower electric power input, i.e., that representing deposition of particles passing through a low-temperature region of the plasma arc. A 3-mm-thick substrate of mild steel was used.

Grinding of the as-sprayed coating with a diamond abrasive wheel at speeds of 20 to 30 ms^{-1} and a radial feed of 0.02 to 0.04 mm was carried out for all specimens. A D-500 Siemens diffractometer was used to perform X-ray diffraction analysis using Co-K_α irradiation.

A Euler four-circle diffractometer was used for the texture measurements. Pole figures of (111), (002), (022), and (113) tetragonal phase of YPSZ and CePSZ were measured and then used for ODF calculations with the Siemens/TEX software. Both ceramics exhibited a very low tetragonal content, and consequently, it was necessary to separate the tetragonal doublet superposition numerically by using a modified Lorentz approximation function and error mean square method. Because the exact values of elastic moduli, S_{hkl}, for tetragonal phase YPSZ and that for CePSZ were not available, then the elastic moduli pertinent to the cubic phase of zirconia[14] were used, i.e., $S^{cubic}_{(200)} \cong S^{tetrag}_{(002),(200)}$, etc.

In the case of X-ray line broadening analysis, instrument correction was performed using the Stockes method[10] and data for pure homogeneous ZrO_2 + 8 wt% Y_2O_3 powder measured under equivalent conditions. However, the acceptability of such a standard quality will be discussed in later sections of this article.

4. Results

4.1 *Phase Analysis*

X-ray diffraction analysis of both ceramics indicated that there are two major phases, i.e., tetragonal and monoclinic, in the as-deposited state. The very low tetragonallity, as expressed by the c/a parameter ratio ($c/a \leq 1.015$), also indicates that the cubic phase might be present. The numerical analysis of superimposed diffraction peaks, where minor cubic peaks should be located between two peaks of tetragonal phase, gave ambiguous results. Therefore, the numeric separation suggested the dominant presence of tetragonal phase and the possible existence of other phases, which were incorporated into an error estimation. The tetragonal lattice parameters of the specimens measured in the as-deposited state are listed in Table 1. There was no evidence of additional phase transformations, such as tetragonal → cubic or tetragonal → monoclinic, which were influenced by the grinding process.

Grinding-induced changes in diffraction peak intensities of the (002)-(200) and (113)-(311) tetragonal doublets are usually indicated by an increasing intensity ratio which is dependent on the testing conditions. However, as can be seen from Tables 2 and 3, the $I_{(022)}/I_{(220)}$ and $I_{(133)}/I_{(331)}$ intensity ratios also changed. However, the grinding-induced changes are not as evident in the above-mentioned tetragonal doublets. Table 2 shows that the measured intensities of the (222) single peak clearly exhibit an influence on the grinding process. This can be considered as either due to texture variation and/or crystal structure changes that would be expressed by a $F_i^2 \cong I_i$ relationship (where F_i is the crystal structure factor).

Table 1 Lattice parameters of tetragonal phases

Specimen	Lattice parameters, nm		
	a	*c*	*c/a*
YPSZ	0.51047 ± 0.00083	0.51470 ± 0.00084	1.0083 ± 0.0023
YPSZ-R	0.51150 ± 0.00003	0.51570 ± 0.00004	1.0082 ± 0.0001
CePSZ	0.51474 ± 0.00026	0.52255 ± 0.00034	1.0152 ± 0.0008

4.2 *Residual Deformation*

Residual normal deformation, ε, measured on (*hkl*) planes of crystals having the particular (*hkl*) planes parallel with the specimen surface and averaged over an effective penetration depth, are shown in Fig. 1. It is evident that ε_L for CePSZ is substantially higher than that of YPSZ-R. The results for YPSZ were virtually identical to those of YPSZ-R. Because the effective X-ray penetration depth (h_e) for each (*hkl*) may be calculated, then the relationship between ε_L and the subsurface depth, also shown in Fig. 1, can also be calculated. It follows that the residual deformation has a tendency to reach zero at some depth, which is a higher magnitude for CePSZ.

4.3 *Microdistortion and Paracrystallinity*

All diffraction peaks of the tetragonal YPSZ and that of CePSZ spectra were used in multiregression analysis using Eq 5 to obtain an estimation of several parameters. This analysis was performed for the YPSZ-R and CePSZ specimens. The measured data along with the proposed model following Eq 5 are shown in Fig. 2 and 3 for both the YPSZ-R and CePSZ ceramics. Table 4 lists the averaged results. Equation 5 agrees with the proposed model. The difference in grinding response of both materials can also be observed. CePSZ has higher distortion in the

Table 2 Normalized X-ray diffraction intensities of individual (*hkl*) peaks

$(hkl)_i$	Normalized intensity, $I_i/I_{i(111)}$					
	YPSZ		YPSZ-R		CePSZ	
	AD	GR	AD	GR	AD	GR
(002)	0.083	0.099	0.076	0.090	0.075	0.109
(200)	0.140	0.131	0.149	0.129	0.140	0.119
(022)	0.437	0.371	0.396	0.364	0.354	0.413
(220)	0.208	0.215	0.245	0.135	0.274	0.153
(113)	0.153	0.164	0.141	0.148	0.141	0.167
(311)	0.304	0.235	0.321	0.228	0.323	0.238
(222)	0.085	0.074	0.092	0.071	0.083	0.068
(133)	...	...	0.132	0.122	0.130	0.105
(331)	...	...	0.089	0.040	0.112	0.097

Note: AD ≡ as-deposited; GR ≡ ground.

Table 3 Grinding-induced diffraction intensity ratios of tetragonal doublets

Intensity ratio	YPSZ		YPSZ-R		CePSZ	
	AD	GR	AD	GR	AD	GR
$I_{(002)}/I_{(200)}$	0.588	0.757	0.509	0.693	0.535	0.918
$I_{(022)}/I_{(220)}$	2.100	2.080	1.610	2.697	1.297	2.751
$I_{(113)}/I_{(311)}$	0.504	0.698	0.441	0.650	0.437	0.704
$I_{(133)}/I_{(331)}$	...	...	1.475	3.084	1.162	1.083

Note: AD ≡ as-deposited; GR ≡ ground.

as-deposited state and also higher elastic distortion after surface grinding because the g_p and σ_L values are greater under these conditions. However, both the YPSZ and CePSZ materials exhibit a randomly distributed paracrystallinity (g_p), which is insensitive to the effect of grinding.

4.4 *Texture ODF*

The major texture components identified in deposited coatings were the {111} fiber and {100} cube fiber, i.e., planes (111) and (100) are parallel to the surface, as can be seen in Fig. 4 to 6.

Comparing ODF of CePSZ and YPSZ in Fig.4 and 5, there is no significant difference between the above-mentioned ideal orientations. The interrelationships among ODFs of individual specimens of CePSZ coatings are also exhibited. On the other hand, the ODF of YPSZ-R, shown in Fig. 6, is very weak and indicates that random crystal orientations are a more characteristic feature. The influence of grinding on given coatings can now also be recognized. Approximately a 50% decrease in volume content of the {111} fiber texture component of the CePSZ coatings is in contrast to a 10% decrease in the case of YPSZ, with little effect for the YPSZ-R coating. A tendency to decrease the amount of the {100} cube fiber texture component under grinding was also indicated.

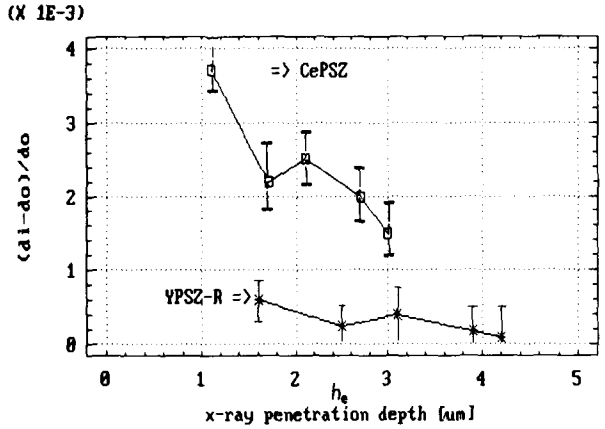

Fig. 1 Residual deformation in surface of plasma-sprayed coating.

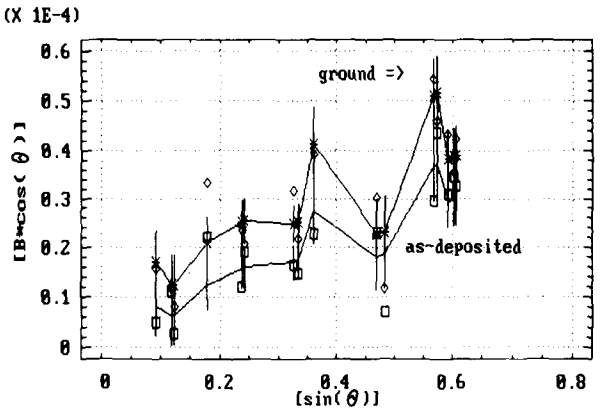

Fig. 2 Regression of Eq 5 with 95% prediction intervals for mean. As-deposited and ground YPSZ-R samples.

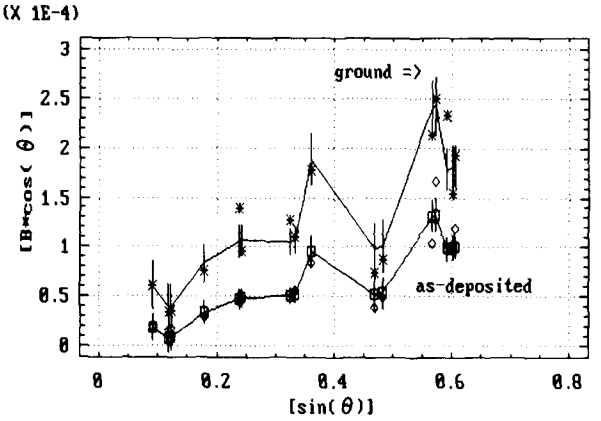

Fig. 3 Regression of Eq 5 with 95% prediction intervals for mean. As-deposited and ground CePSZ samples.

5. Discussion

The plasma-sprayed CePSZ and YPSZ coatings investigated in this work were studied both in their as-deposited and as-ground conditions. Several aspects of the XRD method and interpretation of results are important: First, the level of agreement between these methods and true physical state of ceramic coatings characterized by the distribution of various kinds of imperfections. Second, the limited applicability of some analytical methods that are based on the theory of solid-state physics and models that assume an idealized homogeneous state of the material. It seems evident that a more pragmatic approach, taking into account a balance between both XRD theory and the state of the material, can offer useful results, especially when the results are evaluated with respect to the statistical distribution of errors. In such a way, grinding-induced microstructural changes in ceramic coatings were studied to clarify their nature in terms of a very fine crystal structure. The quantitative estimation of these

Table 4 Results of line broadening multiregression analysis

Ceramic		L, nm	g_p, %	σ_L, MPa
YPSZ-R	As deposited	(a)	1.85 ± 0.10	505 ± 88
	Ground	67 ± 11	1.81 ± 0.10	686 ± 72
CePSZ	As deposited	(a)	2.35 ± 0.05	1391 ± 180
	Ground	43 ± 9	2.43 ± 0.10	2046 ± 174

(a) $[(1/L) \rightarrow 0]$ erroneous estimation at low statistical significance.

effects is influenced by factors such as the primary texture and imperfection distribution. Other factors affecting the intensities of diffraction peaks include mechanisms based on ferroelastic domain switching.[5] However, these cannot be verified without exact knowledge of how the diffraction intensity distribution is controlled by the crystal structure.

The texture existence may be explained by directional crystal growth opposite to the heat flow direction. In light of the ensuing $c \rightarrow t$ transformation, a primary texture is inherited and/or modified into the final major tetragonal phase. Thus, the deposition of partially or completely melted particles is mainly responsible for the primary texture evaluation. If the texture intensity is described quantitatively using ODF (Fig. 4 to 6), then the effect of plasma spray parameters could be registered and under some circumstances also applied for quality control.

Taking into account the decrease in the grinding-induced modification of the ideal {111} fiber orientation ODF, the level of which is different in both CePSZ and YPSZ ceramics, then the increased response in CePSZ could be deduced. On the other hand, the higher mechanical stability of YPSZ and YPSZ-R does not seem to be dependent on the starting ODF texture. This is also consistent with the higher relative residual strain measured in the case of CePSZ (Fig. 1), which was opposite to that of YPSZ-R. Some difference in affected penetration depth can also be assumed.

Analysis of line broadening was able to distinguish not only grinding effects themselves, but also to quantify them using the method proposed by Eq 5 (Table 4). Line broadening with respect to diffraction angle follows the anisotropic S_{hkl} elastic compliances, regardless of their approximation used in this work.

Comparison of the microdistortion and related microstress influenced by anelasticity of both materials shows that CePSZ is at a higher stress level than that of YPSZ. However, the grinding-induced σ_L increase rate for both kinds of materials is nearly the same as the related elastic energy absorbed. The σ_L differences in the as-deposited material (Table 4) are affected by the degree of phase transformation of the particle. The domain size estimation does not agree with literature values, probably because appropriate standards for material and equipment calibration methods are not available. Thus, domain size estimation is a relative measurement. Nevertheless, a decrease in domain size after grinding can be deduced from the results given in Table 4 and indicate that the grinding process evokes a crystal fragmentation like a twinning mechanism.[6]

The observed texture changes, particularly of the {111}⟨uvw⟩ fiber ODF, decrease for CePSZ, and external sur-

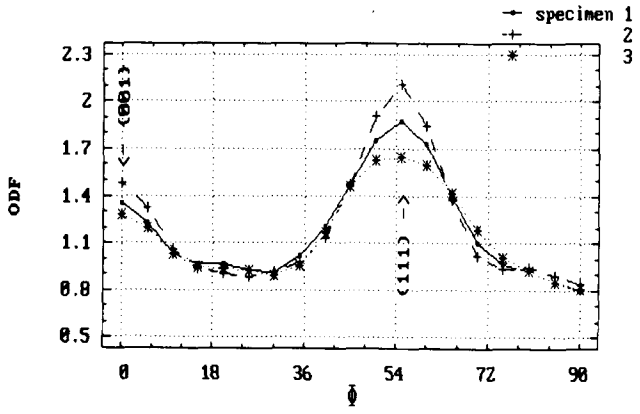

Fig. 4a Texture ODF of as-deposited CePSZ coating. $\phi_1 = 90°$; $\phi_2 = 45°$ (Bunge notation).[15]

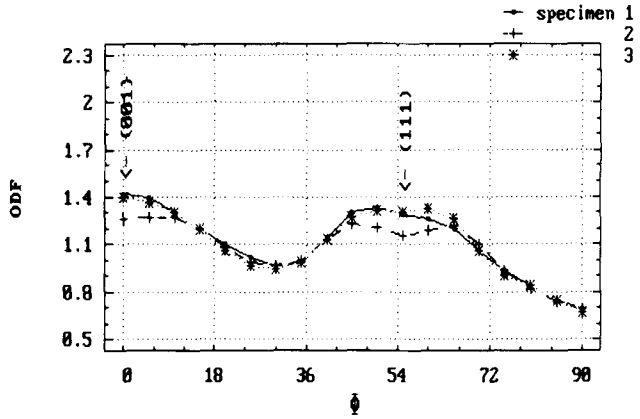

Fig. 4b Texture ODF of the ground CePSZ coating. $\phi_1 = 90°$; $\phi_2 = 45°$.

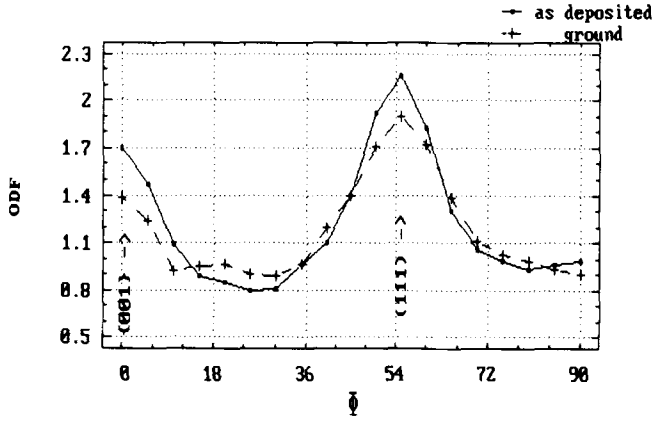

Fig. 5 Texture ODF of the as-deposited and ground YPSZs. $\phi_1 = 90°$; $\phi_2 = 45°$.

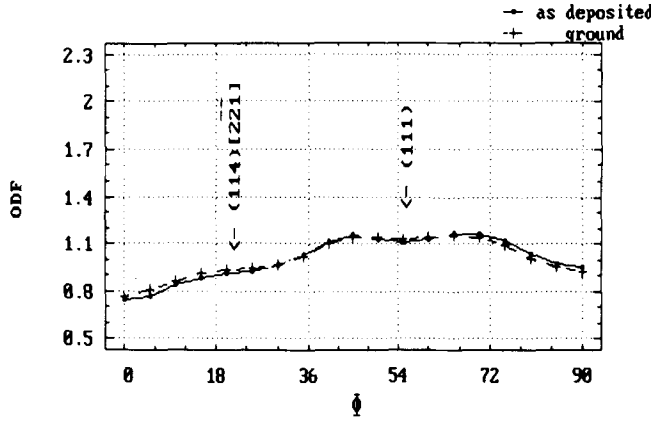

Fig. 6 Texture ODF of as-deposited and ground YPSZ-R samples. $\phi_1 = 90°$; $\phi_2 = 45°$.

face loading stimulates fragmentation and/or domain switching. It is also possible that surface grinding causes an instantaneous temperature rise, which could be sufficient to evoke a transition between brittle and plastic behavior.

6. Conclusion

The results of surface grinding-induced changes in two plasma-sprayed coatings made of CePSZ and YPSZ ceramics, presented in this work, can be summarized as follows. The original texture and heterogeneity in the as-deposited state are influenced by the deposition process. These physical characteristics were evaluated by modification of the X-ray powder diffraction method. The model, which considers anelasticity and paracrystal characteristics in microdistortion fields of polycrystal aggregates, is statistically significant.

The quantitative ODF interpretation of the original and grinding-modified texture was used to recognize different behaviors of the given materials and to examine plasma spray parameters. Such methods may be used for quality control application.

Quantified texture changes have been related to changes in diffraction peak intensities of the tetragonal doublets CePSZ and YPSZ. A mechanism based on domain switching mechanism, as observed in ferroelastic crystals,[3] has been proposed.

The CePSZ ceramic is more sensitive to the grinding process, so that its lower mechanical stability and consequently better surface mechanical properties are opposite to those of YPSZ ceramic.

References

1. A.G. Evans and R.M. Cannon, Toughening of Brittle Solids by Martensitic Transformations, *Acta Metall.*, Vol 3 (No. 5), 1986, p 761-800
2. A.V. Virkar and L.K. Matsumoto, Ferroelastic Domain Switching as a Toughening Mechanism in Tetragonal Zirconia, *J. Am. Ceram. Soc.*, Vol 69 (No. 10), 1986, p C224-C226
3. V.K. Wadhawan, Ferroelasticity and Related Properties of Crystals, *Phase Transitions*, Vol 3 (No. 1), 1982, p 3-103
4. G.V. Srinivasan, J.-F. Jue, S.-Y. Kuo, and A.V. Virkar, Ferroelastic Domain Switching in Polydomain Tetragonal Zirconia Single Crystals, *J. Am. Ceram. Soc.*, Vol 72 (No. 11), 1989, p 2098-2103
5. K. Mehta, J.-F. Jue, and A.V. Virkar, Grinding-Induced Texture in Ferroelastic Tetragonal Zirconia, *J. Am. Ceram. Soc.*, Vol 73 (No. 6), 1990, p 1777-1779
6. J.-F. Jue, J. Chen, and A.V. Virkar, Low-Temperature Aging in t' Zirconia: The Role of Microstructure on Phase Stability, *J. Am. Ceram. Soc.*, Vol 74 (No. 8), 1991, p 1811-1820
7. B.E. Warren and J. Biscoe, *J. Am. Ceram. Soc.*, Vol 21, 1938, p 49
8. R.P.I. Adler, U.M. Otte, and C.N.J. Wagner, Determination of Dislocation Density and Stacking Fault Probability from X-Ray Powder Pattern Peak Profile, *Metall. Trans.*, Vol 1 (No. 9), 1970, p 2375-2382
9. R.L. Rothman and J.B. Cohen, A New Method for Fourier Analysis of Shapes of X-Ray Peaks and Its Application to Line Broadening and Integrated Intensity Measurement, *Advances in X-Ray Analysis*, Vol 12, Plenum Press, 1969, p 208-235
10. C.N.J. Wagner and E.N. Aqua, Analysis of the Broadening of Powder Pattern Peaks from Cold-Worked Face-Centered and Body-Centered Cubic Metals, *Advances in X-Ray Analysis*, Vol 7, Plenum Press, 1963, p 46-65
11. A.M. Hindeleh and R. Hosemann, Paracrystals Representing the Physical State of Matter, *J. Phys. C: Solid State Phys.*, Vol 21, 1988, p 4170-4255
12. W. Vogel and R. Hosemann, Evaluation of Paracrystalline Distortions from Line Broadening, *Acta Crystallogr. A*, Vol 26, 1970, p 272-277
13. J. Zeman and M. Cepera, Report 78-1/742, Material & Technology Institute, Brno, Czech Republik, 1992, in Czech
14. R.P. Ingel and D. Lewis III, Elastic Anisotropy in Zirconia Single Crystals, *J. Am. Ceram. Soc.*, Vol 71 (No. 4), 1988, p 265-271
15. H.J. Bunge, *Methematische Methoden der Texturanalyse* (Mathematical Method of Texture Analysis), Akademie Verlag, Berlin, 1969, in German